# Plastic Behavior of 2024-T3 Under Uniaxial Shear Tests

**Daghfas Olfa, Znaidi Amna, Gahbiche Amen and Nasri Rachid**

**Abstract** The plastic anisotropy of a sheet is measured by performing tension tests as well as by shear tests in different loading directions. In this paper, the main objective is to model the behavior of a 2024 aluminum alloy from experimental simple shear tests from several directions relative to the rolling direction. First, an experimental device of simple shear tests and the studied material are described. Second, the experimental results in terms of hardening curves are presented on three loading directions. In order to further refine the experimental part of this work, microstructural observations were conducted through transmission electronic microscopy (TEM) to show interactions between the precipitates and dislocations in studied material. Finally, several hardening laws are used to describe the isotropic hardening such as Hollomon law, Voce law, and Bron law. By smoothing experimental hardening curves shear stress–shear strain a selection is made in order to choose the most appropriate hardening law to identify the anisotropic parameters of the studied material.

**Keywords** Aluminum alloy · Anisotropy · Simple shear test
Metal sheet · Hardening law

D. Olfa (✉) · Z. Amna · N. Rachid
University of Tunis El Manar, National School of Engineers of Tunis,
LR-MAI-ENIT BP37, 1002 Tunis, Tunisia
e-mail: daghfasolfa@yahoo.fr

Z. Amna
e-mail: Amna.znaidi@Laposte.net

N. Rachid
e-mail: rachidnasri2003@yahoo.fr

G. Amen
Mechanical Engineering Laboratory, National School of Engineers of Monastir,
Monastir, Tunisia
e-mail: amen.gahbiche@yahoo.fr

# 1  Introduction

The simple shear test is recognized as the second test after the simple tensile in the axes, which can be considered, with a good approximation, as homogeneous for certain geometries of specimens. In addition, it makes it possible to achieve fairly large plastic deformations without any localization of the deformation.

Several types of shear mounting have been developed: Miyauchi (1984), G'sell and Rauch (Genevois 1990) and Gary and Nowacki (Gary and Nai 1986).

The shear tests were carried out on a specific device developed by Gahbiche (2006) at the Mechanical Engineering Laboratory [LGM]. This device is an improved version of Miyauchi, Gary, and Nowacki. It is instrumented by an extensometer to measure the relative displacement of the two jaws which is a manifested advantage. It can be considered homogeneous and cyclic shear tests can be realized by reversing the direction of stress. The device is mounted on a tensile machine.

The Portevin Le Chatelier (PLC) effect has been observed in steels and aluminum alloys (Le Chatelier and Portevin 1923; Hopperstad et al. 2006). It is assumed that this effect is due to aging of mobile dislocations during the interaction between them and solute atoms diffusion (Van den Beukel 1975). The bibliography on this subject (Garat et al. 2008; Bouabdallah 2006) approach theoretical aspects as well as experimental ones. A common belief is that the PLC effect exists for tensile tests because of the homogeneous state of stress (Jaoul 2008; Matthieu and Samuel 2011). In fact, they also occur for simple shear curves which are the main basis of this work.

Three isotropic hardening functions are used in this study defined by the Hollomon law with two constants, the Voce law (1948) with three constants and Bron law (2004) with six parameters to be identified from experimental curves. The experimental results obtained are discussed and analyzed in relation to the microstructure of the studied alloy using the TEM.

# 2  Experimental

**Material Testing**

The material used in this investigation is an aluminum alloy (AA2024 in T3 condition) with structural hardening, in the form of a rolled sheet with 1.5 mm thickness. The composition of the studied material according to DIN EN 573 (Develay 1990) is given in Table 1. Young's modulus $E$ is determined as 73 GPa

**Table 1** Chemical composition of 2024-T3

|   | Si | Cu | Mn | Mg | Cr | Zn | Ti | Fe | Al |
|---|----|----|----|----|----|----|----|----|----|
| % | 0.5 | 4.9 | 0.9 | 1.8 | 0.1 | 0.25 | 0.15 | 0.5 | Remainder |

**Table 2** Heat treatment applied to 2024-T3

| Solutionizing | Quenching | Pre-stretching | Maturation |
|---|---|---|---|
| 495 °C (±5 °C) | Water < 40 °C | 2% | Room T° > 4 days |

with Poisson's ratio $\nu = 0.33$. Table 2 presents the heat treatment applied to 2024 alloy.

### Form and dimensions of specimen test

The specimen of the shear test has two useful areas which are similar and their dimensions are $l_o = 28$ mm, $b_o = 3.3$ mm. The shape and the dimensions of specimen shear test are shown in Fig. 1. The thickness of sheet metal $e_0$ is equal to 1.5 mm.

### Experimental set

Uniaxial Shear tests were performed on a specific device (Fig. 2a) developed by Gahbiche (2006) in the laboratory [LGM]. This device is instrumented by an extensometer for measuring the relative displacement of the two jaws.

The device is mounted on a tensile machine (Fig. 2b) with two jaws, one mobile and the other fixed, which clamp the test specimen. The tensile machine imposes the displacement on the mobile jaw in order to create the shear.

The two useful areas of the test specimen have rectangular shapes before the test (Fig. 3a). After the shear test (Fig. 3c), their shapes transformed into parallelograms knowing that the dimensions $l_0$ and $b_0$ remain constant.
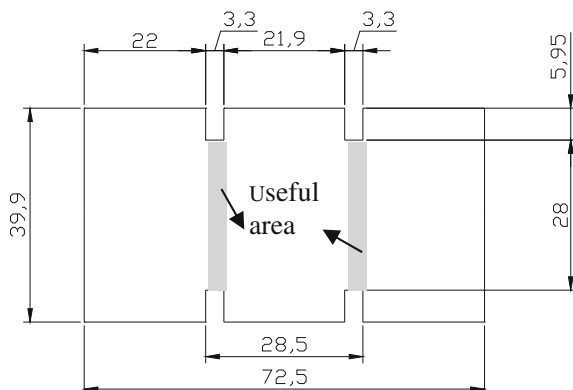
Through the acquisition chain (Fig. 2b) the force F is recorded as a function of the relative displacement $\delta$ between the jaws.

From these results obtained during the shear test, it is possible to express:

- The shear stress $\tau$ which is defined as follows:

$$\tau = \frac{F}{l_0 \cdot e_0} \tag{1}$$

**Fig. 1** Form and dimensions of shear test specimen
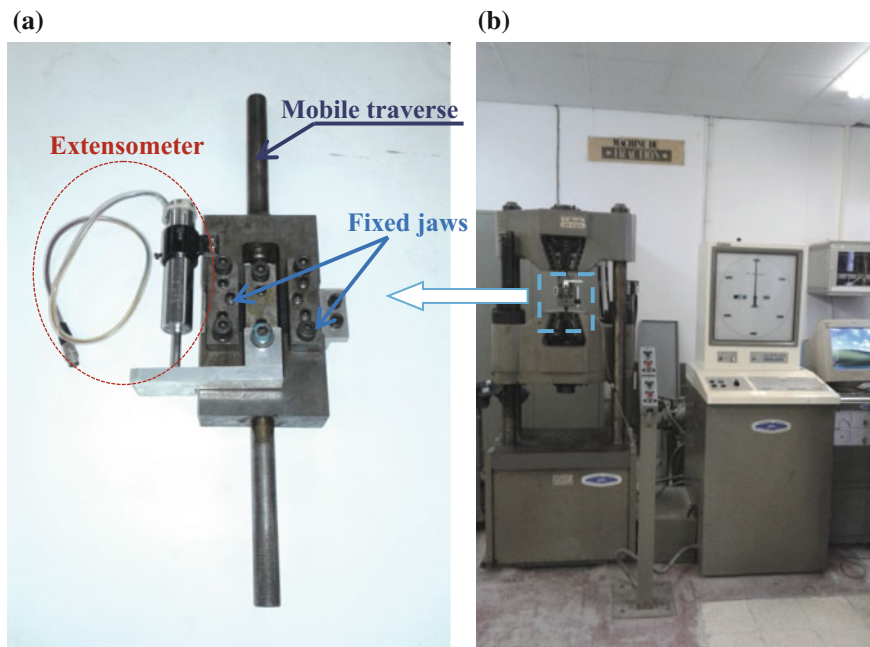
**(a)** **(b)**



**Fig. 2** **a** Specific device of shear test **b** Tensile machine and acquisition chain [LGM]

- The shear strain γ is written in the form:

$$\gamma = \frac{\delta}{b_0} \qquad (2)$$

Microstructural characterization studies were conducted on specimens of 2024 aluminum alloy in rolling direction using a JEOL 2010 transmission electron microscope from the TEMSCAN in Toulouse. The samples about 3 mm diameter and 50 μm thick were obtained and were polished with abrasive papers and attacked with the reagent of the killer.

## 3 Phenomenological Hardening Laws

In the present work, a behavior model is used with different hardening laws. A brief description of their equations and the acronyms that will be used for these models in the presentation of the numerical results are given.
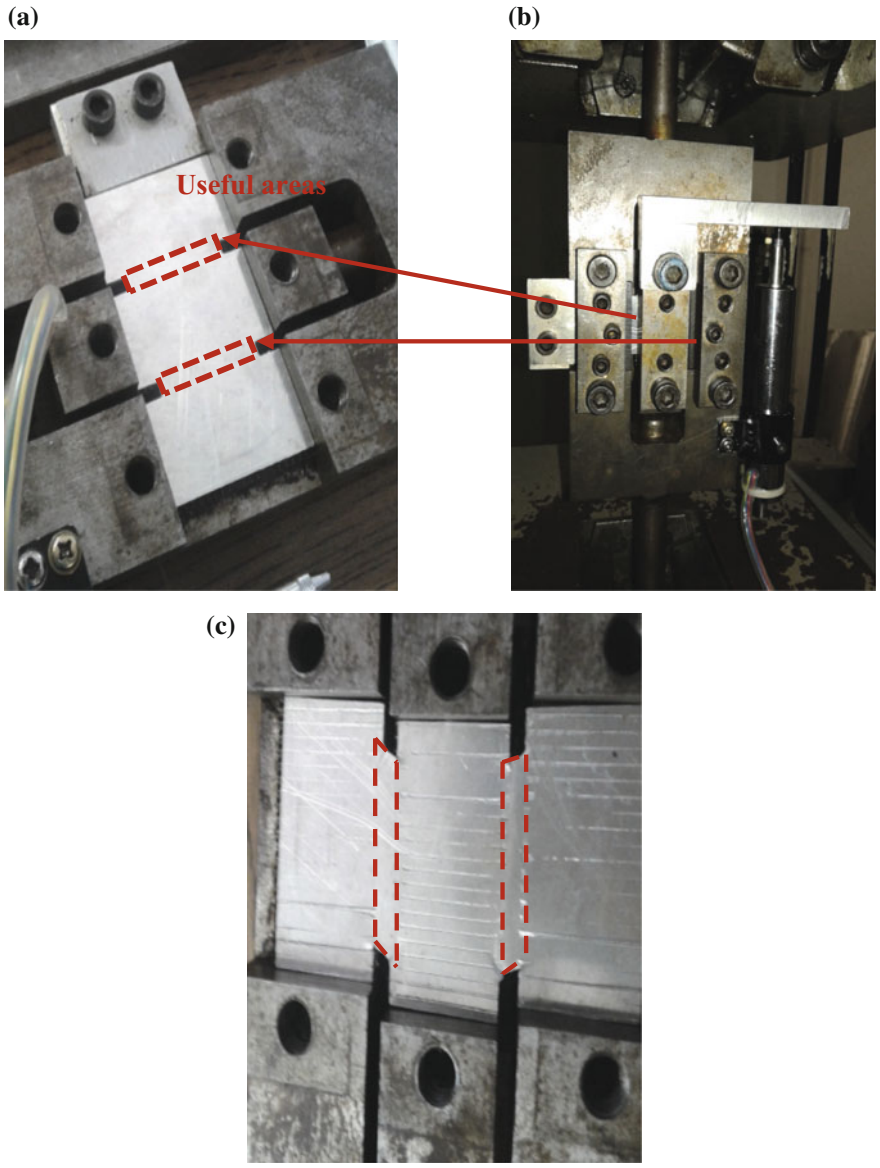
**(a)**

**(b)**



**(c)**

**Fig. 3** Representation of test specimen **a** Before shear test **b** During testing **c** After shear test

Three classical isotropic hardening laws are selected from the literature to describe the plastic behavior of aluminum and its alloys:

(a) The Hollomon law (Holψ°):

Among the most used hardening laws in the literature is the power law named the Hollomon law. It describes very satisfactory the behavior of the pure aluminum in simple tensile (Znaidi et al. 2016).

$$\sigma_s(\varepsilon^p) = k(\varepsilon^p)^n \tag{3}$$

$\sigma_s(\varepsilon^p)$: Isotropic hardening function; where $\varepsilon^p$ is the plastic strain.

This law is based on only two parameters k and n where n is strain hardening exponent.

(b) The Voce law (Voce$\psi°$):

The second law used is the Voce law or the saturation law. Its interest is to represent the change of regime between the linear elastic part and the hardening curve continuously through the use of an exponential.

$$\sigma_s(\varepsilon^p) = \sigma_y(1 - \alpha \exp(\beta\varepsilon^p)) \tag{4}$$

This law introduces a hardening saturation $\sigma_y$, $\alpha$ and $\beta$ describes the nonlinear part of the curve during the onset of plasticity, where $0 < \alpha < 1$ and $\beta < 0$. It describes very satisfactory the hardening curves of the aluminum alloy 7075-T7 in a simple tensile test (Daghfas et al. 2017a, b).

(c) The Bron law (Bron$\psi°$):

This law is proposed by Bron (2004) with six parameters to be identified.

$$\sigma_s(\varepsilon^p) = \sigma_0[1 + K_0\varepsilon^p + K_1(1 - \exp(-k_1\varepsilon^p)) + K_2(1 - \exp(-k_2\varepsilon^p))] \tag{5}$$

It is a modified expression of the Voce law or it contains twice the expression (4). $\sigma 0$ is the yield strength; $K_1 K_2$ is the hardening saturation; $k_1 k_2$ is the description of the nonlinear part of the hardening curve.

## 4 Results and Discussion

### Experimental results

Figure 4 presents the experimental shear curves for three loading directions.

Uniaxial shear curves for three directions from the rolling direction reveal the nature of anisotropy in this material especially in terms of ductility and shear strength that vary with orientation in the plane of the sheet.

It is seen that the shear test achieves more large plastic deformations than the tensile test (Daghfas et al. 2017a, b) without localization of deformation.

According to three loading directions, the slope of strain hardening is different which shows the anisotropy of studied material.
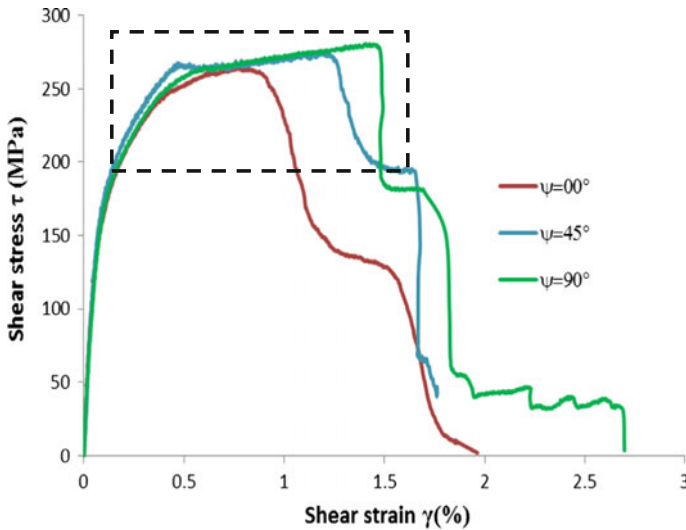
**Fig. 4** Experimental shear stress-shear strain obtained at $\Psi = 00°$ $\Psi = 45°$ $\Psi = 90°$

It has high mechanical properties both in terms of strength and ductility in the transverse direction ($\psi = 90°$) compared to other loading directions ($\psi = 00°$ and $\psi = 45°$).

Figure 5 is obtained by zooming framed area of Fig. 4.

The Portevin–Le Chatelier Phenomenon (PLC) is observed (Fig. 5) which is one of the forms of heterogeneous plastic deformation. It occurs at the macroscopic scale, in the form of localized deformation bands. These experimental results obtained are discussed and analyzed in relation to the microstructure (Fig. 6) of the studied alloy using Transmission Electron Microscopy (TEM).

Figure 6 shows that the structure is heterogeneous with grains containing many dislocations. The rolling operation leads to a flattening of the grains and the distribution of the dispersoids in elongated strips along the rolling direction.

The presence of precipitates and dislocations are very important. This is due to the structural hardening by precipitation applied to the studied material. The dislocations are created during the prestretching operation (Table 2) conducted between quenching and maturation.

The interaction between dislocations and precipitates is realized according to the hardness of the precipitates. As the latter is harder than the matrix of the material the dislocations cannot penetrate the precipitates and shear them. So they are forced to bypass them.

It is noted that the enlargement of the separation between the precipitates deceases their resistance and facilitates their bypass by the dislocations.

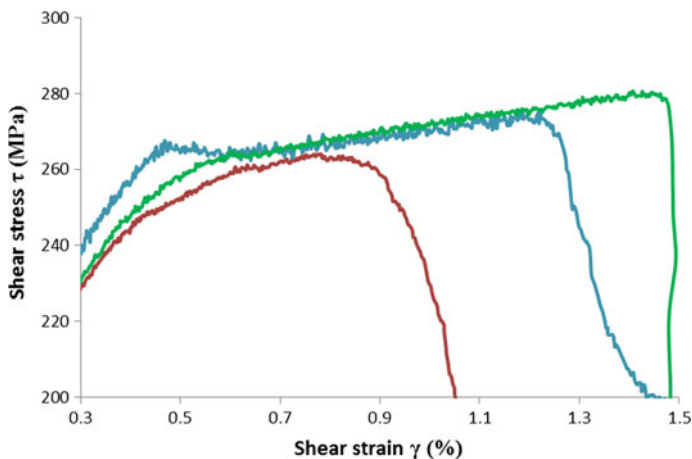Figure 6 shows their interaction which explains the presence of PLC phenomena.
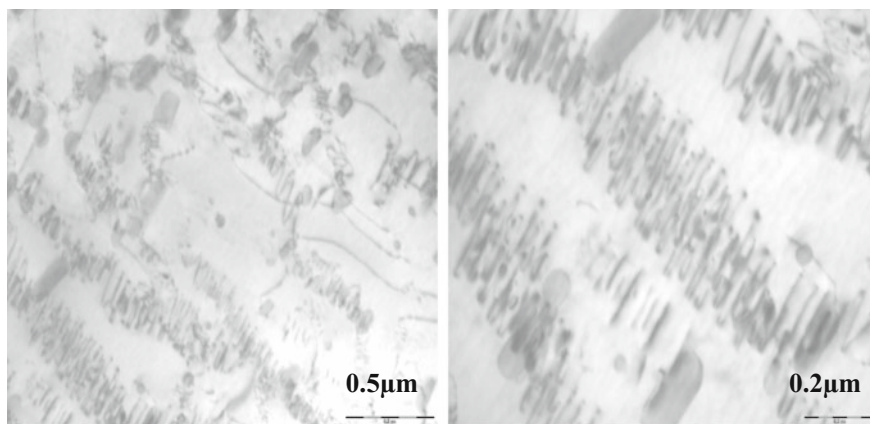
**Fig. 5** Zoom of the framed area of Fig. 4



**Fig. 6** Microstructure of dislocations in 2024-T3 specimen (TEM)

## Identification results

From the experimental results, the hardening curves are fitted using the three laws presented above. These curves allow us to determine the parameters of the different laws (see Table 3) and to choose the most appropriate law to describe the plastic behavior of the studied alloy.

The smoothing returns to choose the parameters of hardening laws while minimizing the quadratic difference between the theoretical and experimental results. The classical hardening laws consist in the adjustment of their functions on experimental curves to identify the unknown parameters (Table 3).

**Table 3** Identified parameters of different hardening laws

| Laws | Parameters | 00° | 45° | 90° |
|------|-----------|------|------|------|
| Hollomon | k | 277.93 | 275.187 | 273.089 |
| | n | 0.1664 | 0.1245 | 0.137 |
| Voce | $\sigma_y$ | 266.22 | 270.3698 | 275.3461 |
| | $\alpha$ | 0.6248 | 0.6456 | 0.6153 |
| | $\beta$ | −5.034 | −5.9044 | −4.4926 |
| Bron | $\sigma_0$ | 31.65 | 35.5934 | 35.5576 |
| | $K_0$ | −0.5938 | −0.0777 | −0.3674 |
| | $K_1$ | 1.4467 | 1.8006 | 1.71 |
| | $K_2$ | 5.434 | 4.871 | 4.612 |
| | $k_1$ | 4.9377 | 324.9938 | 135.7633 |
| | $k_2$ | 8.3112 | 5.6576 | 5.4466 |

The identified curves by Hollomon, Voce, and Bron laws compared to the experimental shear curves obtained in the three loading directions relative to the rolling direction (00°, 45° and 90°) are presented in Fig. 7a, b and c, respectively.

In order to show the most suitable law for the identification of *shear Stress– shear strain curves*, a comparison between three hardening laws is made.
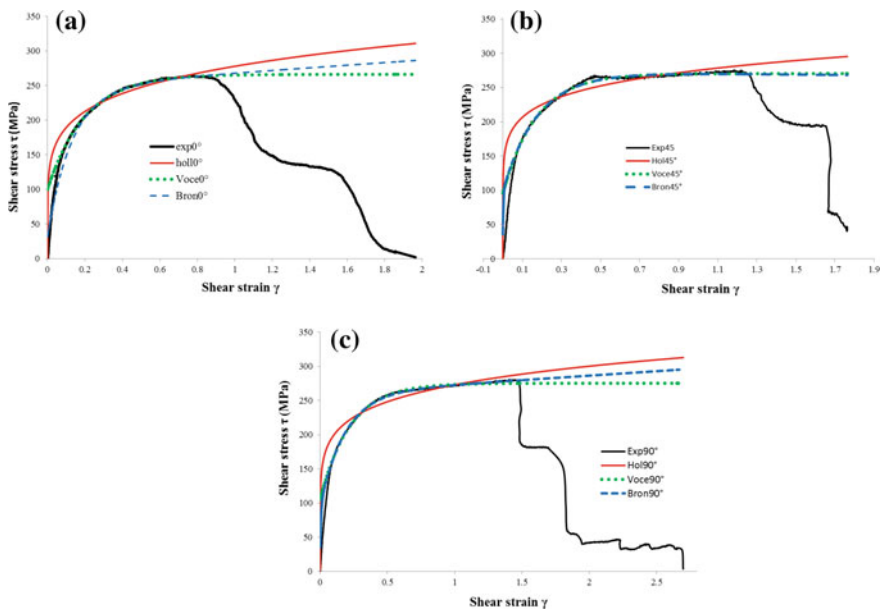


**Fig. 7** Identification of the hardening curve: (a) $\psi = 00°$ (b) $\psi = 45°$ (c) $\psi = 90°$

It is seen that in the plastic deformation part the voce and the Bron laws describe better the hardening curves than the Hollomon law for all loading directions from the rolling direction.

Since the two laws give similar results, the Voce law with fewer parameters is selected subsequently to identify anisotropy behavior in the next work.

# 5  Conclusion

In this study, off—axis shear tests are carried on 2024 aluminum alloy through three loading directions from the rolling direction. These experimental results have allowed to investigate the mechanical properties and to identify the unknown parameters of different isotropic hardening laws. By comparing these latter laws, it is shown that Voce law and Bron law lead to a good description of the shear stress–shear strain curves. However, Voce hardening law may be sufficient to correctly describe the hardening of the aluminum alloy in uniaxial test. The Portevin–Le Chatelier phenomenon observed in hardening curves is explained by the interaction between dislocation and precipitates presented by images of transmission electron microscopy.

# References

Bouabdallah K (2006) Caractérisation de l'effet Portevin-Le Chatelier dans les alliages aluminium magnésium - Apport des techniques d'analyse d'images. Mécanique [physics.med-ph]. Université de Savoie Français

Bron F (2004) Ductile tearing thin 2024 aluminum alloy sheets for aeronautical application. PhD thesis, National school of Mines of Paris

Daghfas O, Znaidi A, Ben Mohamed A, Nasri R (2017a) Experimental and numerical study on mechanical properties of aluminum alloy under uniaxial tensile test. Frattura ed Integrità Strutturale 39:271–282

Daghfas O, Znaidi A, Guahbiche A, Nasri R (2017b) Plastic behavior laws of aluminum aerospace alloys: experimental and numerical study. J Theor Appl Mech (In review)

Develay R (1990) Properties of aluminum and aluminum alloys (French) Technical Engineer. Report M440

Gahbiche A (2006) Caracterisation expérimentale des tôles d'emboutissage, application a l'identification des lois de comportement. PhD thesis, National School of Engineers of Monastir, Tunisia

Garat V, Cloue JM, Poquillon D, Andrieu E (2008) Influence of Portevin-Le Chatelier effect on rupture mode of alloy 718 specimens. J Nuclear Mater 375:95–101

Gary G, Nai K (1986) Description d'un essai de cisaillement simple. J de Physique IV-C8

Genevois P (1990) Étude expérimentale du comportement des tôles minces sollicités en chargements simples et complexes. Rapport IRSID, RI 91317

Hopperstad OS, Borvik T, Berstad T, Benallal A (2006) Finite element simulations of the Portevin-Le Chatelier effect in aluminium alloy. J Phys IV 134:435–441

Jaoul B (2008) Etude de la plasticité et application aux métaux. Réédité par Les Presses des Mines, Paris

Le Chatelier F, Portevin A (1923) Sur le phénomène observé lors de l'essai de traction d'alliages en cours de transformation. C R Acad Sci Paris 176:507–510

Matthieu M, Samuel F (2011) Le calcul de structures en présence de vieillissement statique ou/et dynamique d'alliages métalliques. 20ème Congrès Français de Mécanique, CFM 2011, Besançon, France

Miyauchi K (1984) A proposal of a planar simple shear test in sheet metals. Sci paper of IPCR 78

Van den Beukel A (1975) Theory of the effect of dynamic strain aging on mechanical properties. Phys Status Solidi 30:197. https://doi.org/10.1002/pssa.2210300120

Voce E (1948) The relationship between stress and strain for homogeneous deformations. J Inst Metals 74:537–562

Znaidi A, Daghfas O, Gahbiche A, Nasri R (2016) Identification strategy of anisotropic behavior laws: application to thin sheets of A5. J Theor Appl Mech 54:1147–1156